

Electronic Supplementary Information

Low band gap conjugated polymers combining siloxane-terminated side chain and alkyl side chain: a side chain engineering achieving large active layer processing window for PCE>10% in polymer solar cells

Xuncheng Liu,^{‡a} Li Nian,^{‡a} Ke Gao,^{‡a} Lianjie Zhang,^a Lechi Qing,^a Zhen Wang,^a Lei Ying,^a Zengqi Xie,^{*a} Yuguang Ma,^a Yong Cao,^a Feng Liu^{*b} and Junwu Chen^{*a}

^a *Institute of Polymer Optoelectronic Materials & Devices, State Key Laboratory of Luminescent Materials & Devices, South China University of Technology, Guangzhou 510640, P. R. China. E-mail: psjwchen@scut.edu.cn; msxiez@scut.edu.cn*

^b *Department of Physics and Astronomy, Shanghai Jiaotong University, Shanghai 200240, P. R. China. E-mail: fengliu82@sjtu.edu.cn*

[‡] These authors contributed equally.

1. General Information.

All reagents and solvents, unless otherwise specified, were purchased from Aldrich, Acros, and Alfa Aesar and were used as received. All the solvents used were purified prior to use according to normal procedure. All manipulations involving air-sensitive reagents were performed under an atmosphere of dry argon.

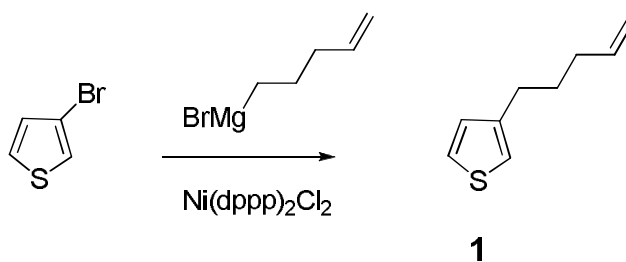
¹H and ¹³C NMR spectra were recorded on a Bruker AVANCE Digital 300 MHz or 500 MHz spectrometer with tetramethylsilane (TMS) as the internal reference. The elemental analysis results of polymers were measured by a Vario EL cube elemental analyzer. Molecular weights of the polymers were obtained on a PL GPC 220 (Polymer Laboratories) at 140 °C using a calibration curve of polystyrene standards, with 1,2,4-trichlorobenzene as the eluent. Thermogravimetric (TGA) measurements were carried out with a NETZSCH (TG209F1) apparatus at a heating rate of 20 °C /min under a nitrogen atmosphere. UV-vis absorption spectra were recorded on a HP 8453 spectrophotometer. Cyclic voltammetry (CV) was carried out on a CHI660A electrochemical workstation with platinum electrodes at a scan rate of 50 mV s⁻¹ against an Ag/Ag⁺ reference electrode with nitrogen-saturated solution of 0.1 M tetrabutylammonium hexafluorophosphate (Bu₄NPF₆) in acetonitrile (CH₃CN). Potentials were referenced to the ferrocenium/ferrocene couple by using ferrocene as an internal standard. Tapping-mode atomic force microscopy (AFM) images were obtained using a NanoScope NS3A system (Digital Instrument). Transmission electron microscopy (TEM) images were obtained using JEM-2100F with an accelerating voltage of 30 kV.

2. Synthesis Procedures

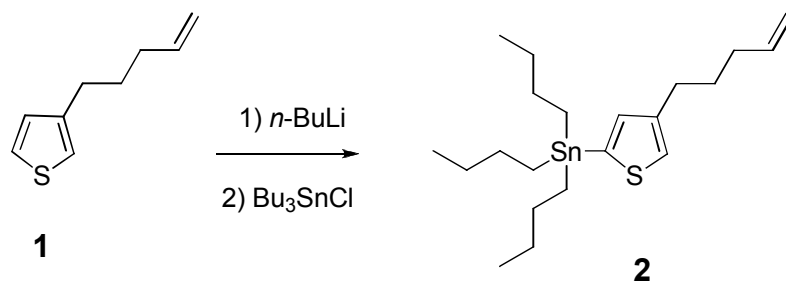
Compounds 4,7-dibromo-5,6-difluoro[2,1,3]benzothiadiazole,

4,7-bis(5-bromo-4-(2-decyltetradecyl)thiophen-2-yl)-5,6-difluoro[2,1,3]benzothiadiazole

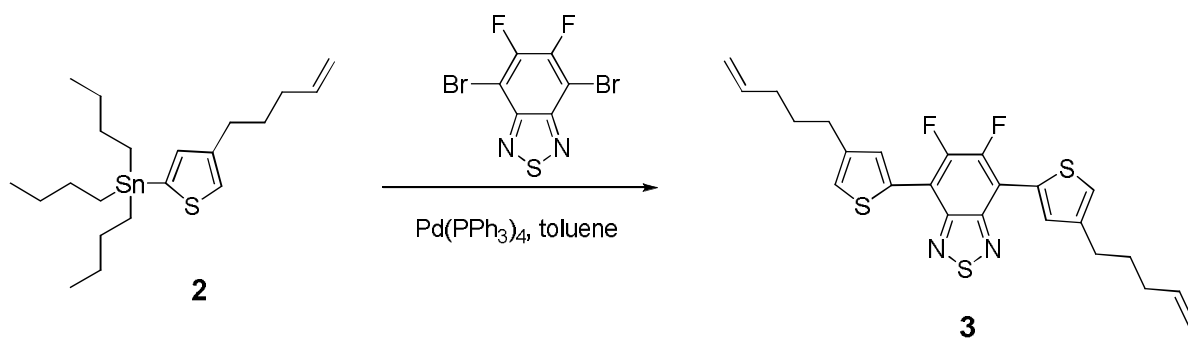
(**FBT2T-C24-Br**), and 5,5'-bis(trimethylstannyl)-2,2'-bithiophene (**2T-SnMe₃**) were prepared according to the literature.¹ The detailed synthesis procedures of the intermediates and the targeted polymers were described below.



3-(Pent-4-en-1-yl)thiophene (1). In a 250 mL two-neck round-bottom flask, Mg (2.4 g, 100 mmol) and a little iodine was dissolved in 150 mL of anhydrous THF under argon protection. The mixture was slightly heated and slowly added 5-bromopent-1-ene (11.9 g, 80 mmol) in 20 min. Then the solution was stirred at 80 °C for 2.5 h and then cooled down to 0 °C. The mixture was added slowly into a solution of 3-bromothiophene (12.2 g, 75 mmol), Ni(dppp)₂Cl₂ (100 mg) at −10 °C in a 500 mL two-neck round-bottom flask. Then the solution was return to room temperature and kept stirring for 12 h. Ethyl acetate was added to extract the organic part. The ethyl acetate phase was washed with brine, dried with anhydrous MgSO₄, and then the solvent was removed under vacuum. The crude product was purified by column chromatography (silica gel, petroleum ether as eluent) to yield 9.3 g (82%) of the product as pale yellow oil. ¹H NMR (500 MHz, CDCl₃) δ 7.29 (s, 1H), 6.98 (d, *J* = 1.5 Hz, 2H), 5.99–5.79 (m, 1H), 5.18–4.91 (m, 2H), 2.70 (t, *J* = 7.6 Hz, 2H), 2.15 (q, *J* = 7.1 Hz, 2H), 1.85–1.72 (m, 2H). ¹³C NMR (126 MHz, CDCl₃) δ 142.70, 138.48, 128.20, 125.13, 119.97, 114.73, 33.27, 29.66, 29.60.

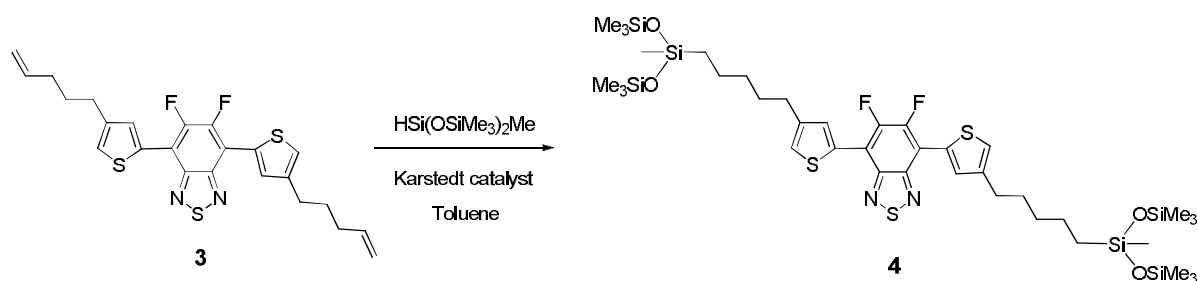


Tributyl(4-(pent-4-en-1-yl)thiophen-2-yl)stannane (2). In a 250 mL two-neck round-bottom flask, 3-(pent-4-en-1-yl)thiophene **1** (7.6 g, 50 mmol) was dissolved in 150 mL of anhydrous THF. *n*-BuLi (2.5 M in hexane) (22 mL, 55 mmol) was added slowly in 10 min under argon protection at -78°C . The solution was stirred for 2 h, and then tributyltin chloride (16 mL, 60 mmol) was added slowly in 10 min. The mixture was gradually returned to room temperature and kept stirring for 12 h. Ethyl acetate was added to extract the organic part. The ethyl acetate phase was washed with brine, dried with anhydrous MgSO_4 , and then the solvent was removed under vacuum to get the crude product as yellow oil, which was used without further purification.



5,6-Difluoro-4,7-bis(4-(pent-4-en-1-yl)thiophen-2-yl)benzothiadiazole (3). In a 100 mL two-neck round-bottom flask, 4,7-dibromo-5,6-difluoro[2,1,3]benzothiadiazole (1.65 g, 5 mmol) and tributyl(4-(pent-4-en-1-yl)thiophen-2-yl)stannane **2** (8.826 g, ~20 mmol) were dissolved in anhydrous toluene (30 mL). The solution was purged with argon for 30 min and tetrakis(triphenylphosphine)palladium (20 mg) was added at room temperature under argon

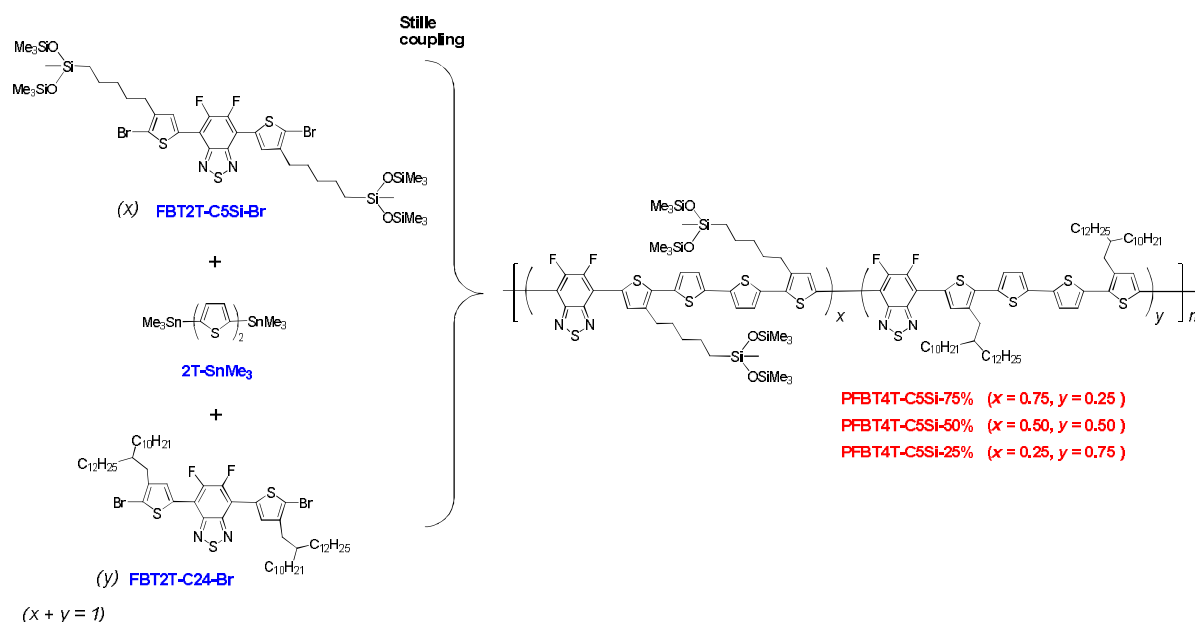
protection. The mixture was heated up to 130 °C for 2 days. The solvent was evaporated under a vacuum, and the crude product was purified by column chromatography (silica gel, petroleum ether/ dichloromethane, 4:1, as eluent) to yield 1.91 g (81%) of the product as a yellow solid. ^1H NMR (500 MHz, CDCl_3) δ 8.11 (d, J = 1.1 Hz, 2H), 7.21 (d, J = 1.0 Hz, 2H), 5.87 (dd, J = 17.0, 10.3 Hz, 2H), 5.09–5.00 (m, 4H), 2.75–2.72 (m, 4H), 2.17 (dd, J = 14.3, 7.1 Hz, 4H), 1.83–1.80 (m, 4H). ^{13}C NMR (126 MHz, CDCl_3) δ 150.84, 148.85, 143.15, 138.40, 132.16, 131.28, 124.11, 114.92, 111.61.



5,6-Difluoro-4,7-bis(4-(5-(1,1,1,3,5,5,5-heptamethyltrisiloxy)pentyl)thiophen-2-yl)benzothiadiazole (4). In a 50 mL two-neck round-bottom flask, 5,6-difluoro-4,7-bis(4-(pent-4-en-1-yl)thiophen-2-yl)benzothiadiazole **3** (1.41 g, 3 mmol) and 1,1,1,3,5,5,5-heptamethyltrisiloxane (1.66 g, 7.5 mmol) were dissolved in anhydrous toluene (25 mL), followed by the addition of a drop of Karstedt's catalyst. The mixture was heated up to 75 °C for 12 h under argon protection. The solvent was evaporated under a vacuum, and the crude product was purified by column chromatography (silica gel, petroleum ether/dichloromethane, 5:1, as eluent) to yield 2.34 g (85%) of the product as a yellow solid. ^1H NMR (500 MHz, CDCl_3) δ 8.12 (s, 2H), 2.71 (t, J = 7.7 Hz, 4H), 1.75–1.67 (m, 4H), 1.44–1.35 (m, 8H), 0.55–0.41 (m, 4H), 0.09 (s, 36H), 0.01 (s, 6H). ^{13}C NMR (126 MHz, CDCl_3) δ 150.87, 148.91, 143.68, 132.23, 131.19, 123.92, 111.66, 33.04, 30.49, 29.07, 23.04, 17.63, 1.86, –0.27.



6

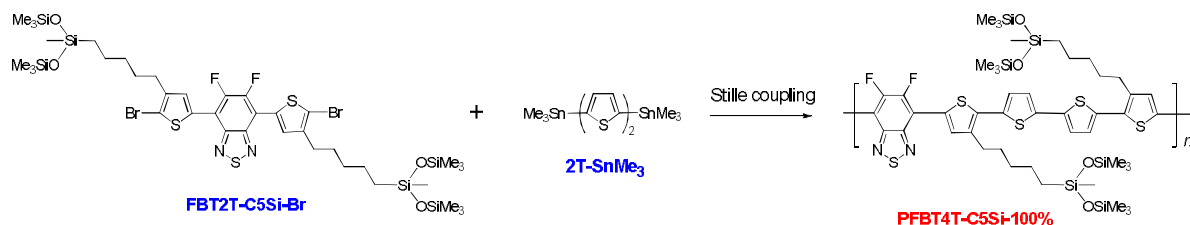


PFBT4T-C5Si-25%. Carefully purified **FBT-C5Si-Br** (161 mg, 0.15 mmol), **FBT-C24-Br** (525 mg, 0.45 mmol), **2T-SnMe₃** (295 mg, 0.6 mmol), Pd₂(dba)₃ (11 mg), and tri(o-tolyl)phosphine (15 mg) were dissolved in chlorobenzene (10 mL). The solution was refluxed with vigorous stirring for 72 h. At the end of polymerization, a small amount of 2-tributylstannylthiophene was added as a monofunctional end-capping reagent to remove bromine end groups, and bromobenzene was added as a monofunctional end-capping reagent to remove trimethylstannum end group. The mixture was then poured into vigorously stirred methanol. The precipitated solid was placed in a Soxhlet thimble, and extracted consecutively with methanol, ethyl acetate, acetone, chloroform, and chlorobenzene. Then the chlorobenzene fraction was concentrated, precipitated in methanol at room temperature, and then filtered and dried in vacuum at 50 °C for 2 days to give 614 mg of final product as a black solid in a yield of 93%. Elemental analysis: calculated: C, 66.88%; H, 8.37%; N, 2.44%; S, 13.95%. Found: C, 66.83%; H, 8.42%; N, 2.31%; S, 13.65%. High temperature GPC (1,2,4-trichlorobenzene, 140 °C): M_n , 105.6 Kg/mol; M_w/M_n , 2.14.

PFBT4T-C5Si-50%. Carefully purified **FBT-C5Si-Br** (322 mg, 0.3 mmol),

FBT-C24-Br (350 mg, 0.3 mmol), **2T-SnMe₃** (295 mg, 0.6 mmol), Pd₂(dba)₃ (11 mg), and tri(o-tolyl)phosphine (15 mg) were dissolved in chlorobenzene (10 mL). Further operation and purification were similar to the synthesis of PFBT4T-C5Si-25%. Finally the chlorobenzene fraction was concentrated, precipitated in methanol at room temperature, and then filtered and dried in vacuum at 50 °C for 2 days to give 588 mg of final product as a black solid in a yield of 91%. Elemental analysis: calculated: C, 61.82%; H, 7.78%; N, 2.49%; S, 14.23%. Found: C, 62.04%; H, 7.95%; N, 2.41%; S, 14.25%. High temperature GPC (1,2,4-trichlorobenzene, 140 °C): *M_n*, 99.8 Kg/mol; *M_w*/*M_n*, 2.38.

PFBT4T-C5Si-75%. Carefully purified **FBT-C5Si-Br** (484 mg, 0.45 mmol), **FBT-C24-Br** (175 mg, 0.15 mmol), **2T-SnMe₃** (295 mg, 0.6 mmol), Pd₂(dba)₃ (11 mg), and tri(o-tolyl)phosphine (15 mg) were dissolved in chlorobenzene (10 mL). Further operation and purification were similar to the synthesis of PFBT4T-C5Si-25%. Finally the chlorobenzene fraction was concentrated, precipitated in methanol at room temperature, and then filtered and dried in vacuum at 50 °C for 2 days to give 524 mg of final product as a black solid in a yield of 83%. Elemental analysis: calculated: C, 56.60%; H, 7.08%; N, 2.54%; S, 14.53%. Found: C, 56.93%; H, 7.32%; N, 2.46%; S, 14.83%. High temperature GPC (1,2,4-trichlorobenzene, 140 °C): *M_n*, 44.0 Kg/mol; *M_w*/*M_n*, 2.03.



PFBT4T-C5Si-100%. Carefully purified **FBT-C5Si-Br** (645 mg, 0.6 mmol), **2T-SnMe₃** (295 mg, 0.6 mmol), Pd₂(dba)₃ (11 mg), and tri(o-tolyl)phosphine (15 mg) were dissolved in

chlorobenzene (10 mL). Further operation and purification were similar to the synthesis of PFBT4T-C5Si-25%. Finally the chlorobenzene fraction was concentrated, precipitated in methanol at room temperature, and then filtered and dried in vacuum at 50 °C for 2 days to give 482 mg of final product as a black solid in a yield of 78%. Elemental analysis: calculated: C, 51.11%; H, 6.43%; N, 2.59%; S, 14.83%; Found: C, 52.36%; H, 6.91%; N, 2.24%; S, 14.99%. High temperature GPC (1,2,4-trichlorobenzene, 140 °C): M_n , 22.0 Kg/mol; M_w/M_n , 2.09.

3. Grazing Incidence X-Ray Diffraction (GIXD) Characterization.

GIXD characterization of the thin films was performed at Advanced Light Source on beamline 7.3.3, Lawrence Berkeley National Lab (LBNL). Thin film samples were prepared on wafer substrates. The scattering signal was recorded on a 2D detector (Pilatus 2M) with a pixel size of 0.172 mm by 0.172 mm. The samples were ~15 mm long in the direction of the beam path, and the detector was located at a distance of ~300 mm from the sample center (distance calibrated using a silver behenate standard). The incidence angle of 0.16° was chosen which gave the optimized signal-to-background ratio. The beam energy was 10 keV, operating at top-off mode. Typically, 10 s exposure time was used to collect diffraction signals. All GIXD experiments were done in helium atmosphere. The data was processed and analyzed using Nika software package.

4. Resonant Soft X-Ray Scattering (RSoXS) Characterization.

RSoXS was performed at Advanced Light Source on beamline 11.0.1.2, Lawrence Berkeley National Lab (LBNL). Thin film samples were spin-casted on the top of the

PEDOT:PSS covered SiO₂ wafers. After that, the BHJ composite films were spin-casted on the top of the SiO₂/PEDOT:PSS substrates under exactly the same conditions as those for the fabrication of solar cell devices. Then BHJ thin films were floated from pure water and transferred onto Si₃N₄ substrates. The scattering signals were collected in vacuum using Princeton Instrument PI-MTE CCD camera.

5. Fabrication and Characterization of Field-Effect Transistors (OFETs).

The top-contacts, bottom-gate organic field-effect transistors were fabricated by conventional techniques using heavily doped Si as the gated electrode, Au as both source and drain electrodes. The surface of the SiO₂ dielectric layer on the wafer was modified by *n*-octadecyltrimethoxysilane (OTS).² Polymer solutions and wafer substrates were pre-heated at 90 °C before spinning. Thin films (~50 nm in thickness) of polymers were formed by spin-coating the hot *o*-dichlorobenzene solutions (5 mg/mL) and annealed at different temperatures for 10 min under nitrogen atmosphere. Gold source and drain contacts (40 nm in thickness) were deposited by vacuum evaporation on the organic layer through a shadow mask. Electrical measurements of devices were carried in a clean and shield box under air at room temperature. The field-effect mobility ($\mu_{\text{h-OFET}}$) was calculated in the saturation regime by using the equation $I_{\text{DS}} = (\mu_{\text{h-OFET}}WC_i/2L)(V_{\text{G}} - V_{\text{Th}})^2$, where I_{DS} is the drain-source current, W is the channel width (500 μm), L is the channel length (30 μm), C_i is the capacitance per unit area of the gate dielectric layer, V_{G} is the gate voltage, and V_{Th} is threshold voltage.

6. Fabrication and Characterization of Polymer Solar Cells (PSCs).

Patterned ITO-glass substrates were used as the cathode in the polymer solar cells. The ITO coated glass substrates were cleaned by sonication in detergent, deionized water, acetone, and isopropyl alcohol and dried in a nitrogen stream. The cathode interlayer ZnO:PBI-H (30nm) were prepared according to the reference.³ The substrates were then transferred into a nitrogen-filled glove box. Active layer solutions (D/A ratio of 1:1.5) with different donor concentrations were prepared in CB:DCB=1:1 with 3% (volume fraction) of DIO. Warm solutions (90 °C) were then spin-coated onto the substrates and dried at 80 °C for 5 min. A 10 nm MoO₃ layer and a 100 nm Al layer were subsequently evaporated through a shadow mask to define the active area of the devices (6.8 mm²) and form the top anode. All device fabrication processes were carried out in a N₂-filled glove box (Braun GmbH). The PCE was determined from $J-V$ curve measurements (using a Keithley 2400 sourcemeter) under a 1 sun, AM 1.5G spectrum from a solar simulator (Oriel model 91192; 1000 W m⁻²). Masks made using laser beam cutting technology to have a well-defined area of 6.8 mm² were attached to define the effective area for accurate measurement. All the masked and unmasked tests gave consistent results with relative errors within 5%. The solar simulator illumination intensity was determined using a monocrystal silicon reference cell (Hamamatsu S1133, with KG-5 visible color filter) calibrated by the National Renewable Energy Laboratory (NREL). Theoretical J_{sc} values obtained by integrating the product of the EQE with the AM 1.5G solar spectrum agreed with the measured value to within 4%.

7. Space-Charge Limited Current (SCLC) Measurement

Hole-only and electron-only devices were fabricated to measure the hole and electron mobilities of active layers using the space charge limited current (SCLC) method with hole-only device of ITO/PEDOT:PSS/neat polymer film or polymer:PC₇₁BM blend film/MoO₃/Al and electron-only device of ITO/Al/ polymer:PC₇₁BM blend film /Ca/Al. The mobilities (μ_{h-SCLC} or μ_{e-SCLC}) were determined by fitting the dark current to the model of a single carrier SCLC, described by the equation:

$$J = \frac{9}{8} \epsilon_0 \epsilon_r \mu \frac{V^2}{d^3}$$

where J is the current, E is the effective electric field, ϵ_0 is the permittivity of free space, ϵ_r is the material relative permittivity, d is the thickness of the active layer, and V is the effective voltage. The effective voltage can be obtained by subtracting the built-in voltage (V_{bi}) from the applied voltage (V_{appl}), $V = V_{appl} - V_{bi}$. The mobility can be calculated from the slope of the $J^{1/2} \sim V$ curves.

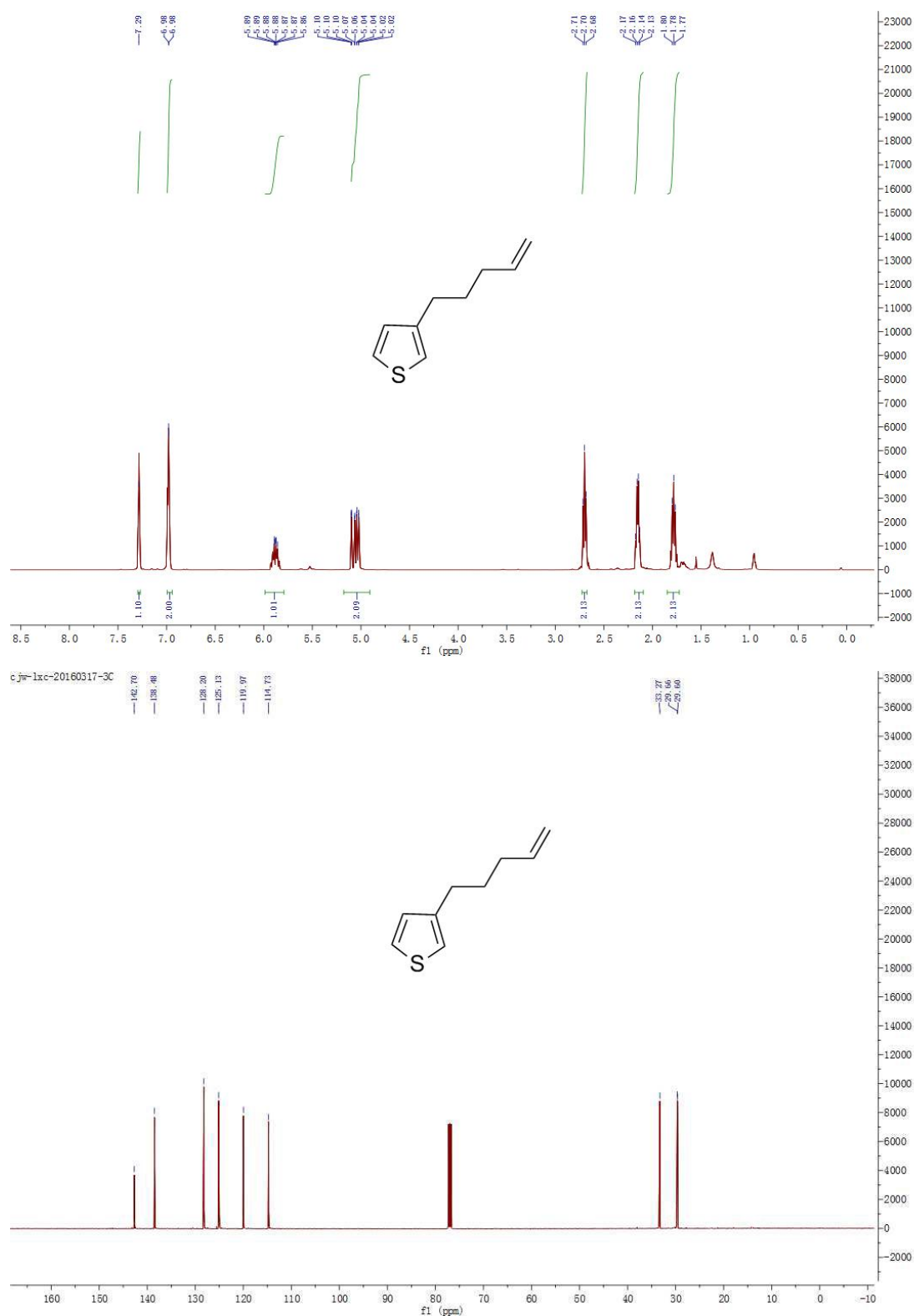


Fig. S1 ¹H NMR and ¹³C NMR spectra of compound **1** in CDCl₃.

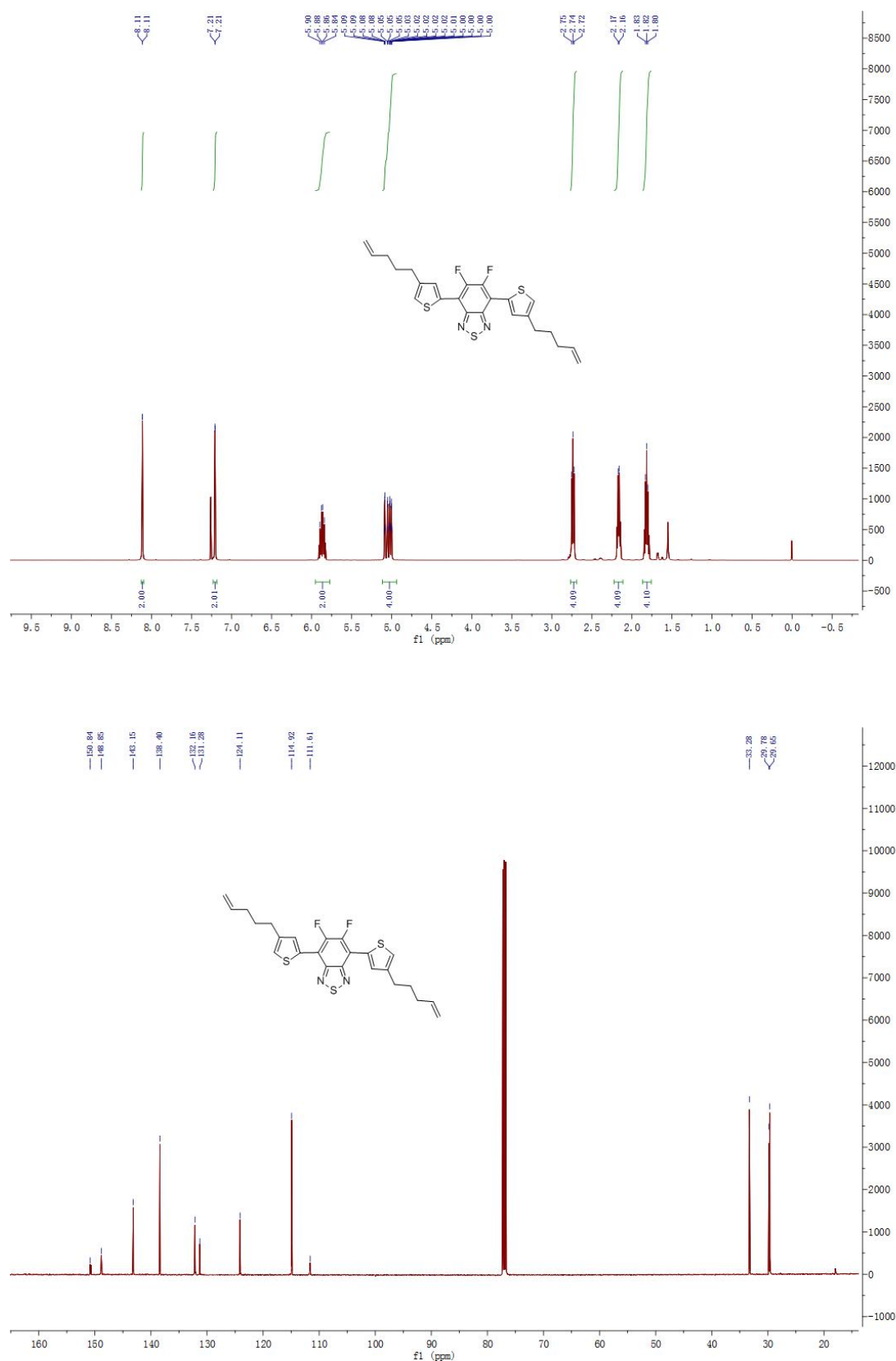


Fig. S2 ^1H NMR and ^{13}C NMR spectra of compound **3** in CDCl_3 .

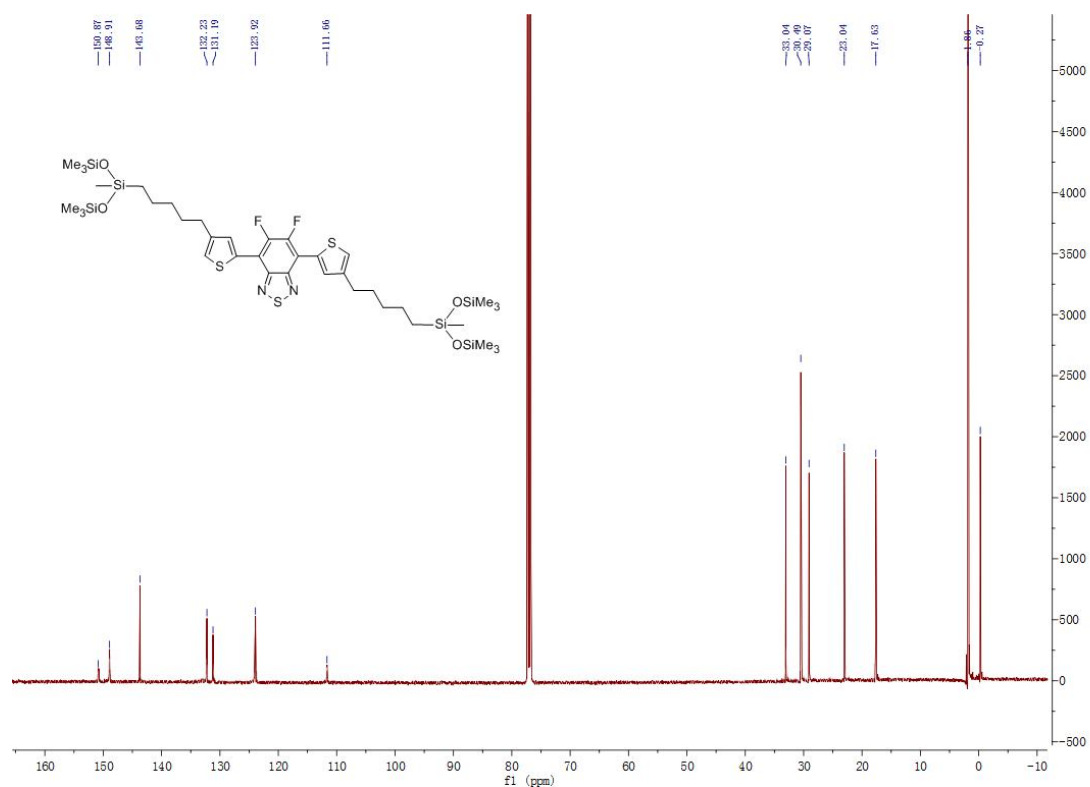
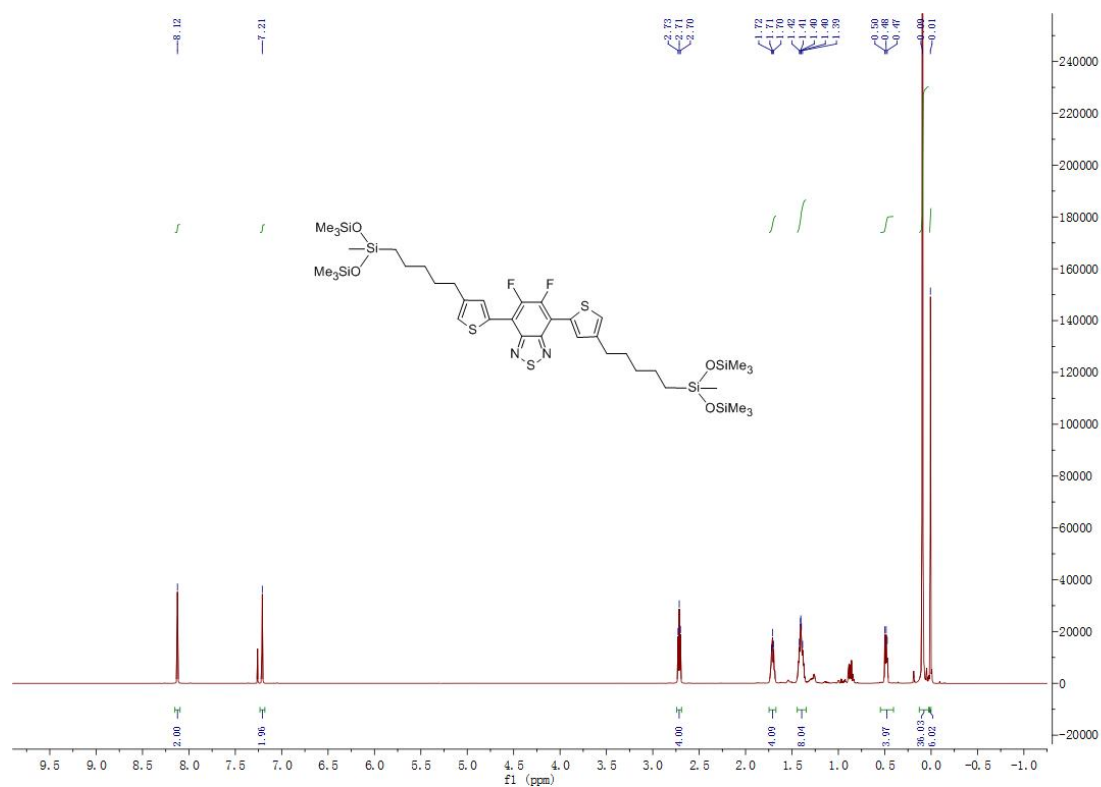


Fig. S3 ¹H NMR and ¹³C NMR spectra of compound **4** in CDCl₃.

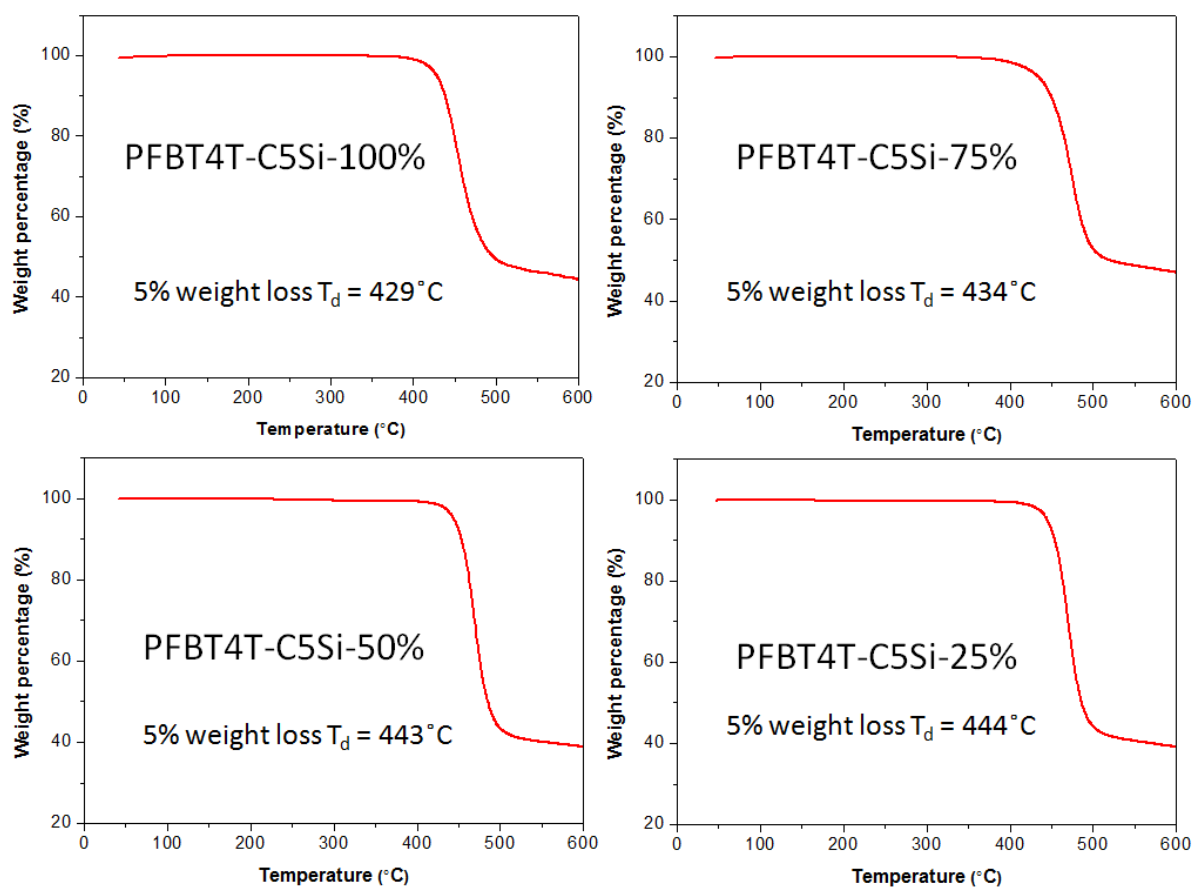


Fig. S5 Thermogravimetric analysis (TGA) for PFBT4T-C5Si-100%, PFBT4T-C5Si-75%, PFBT4T-C5Si-50%, and PFBT4T-C5Si-25%.

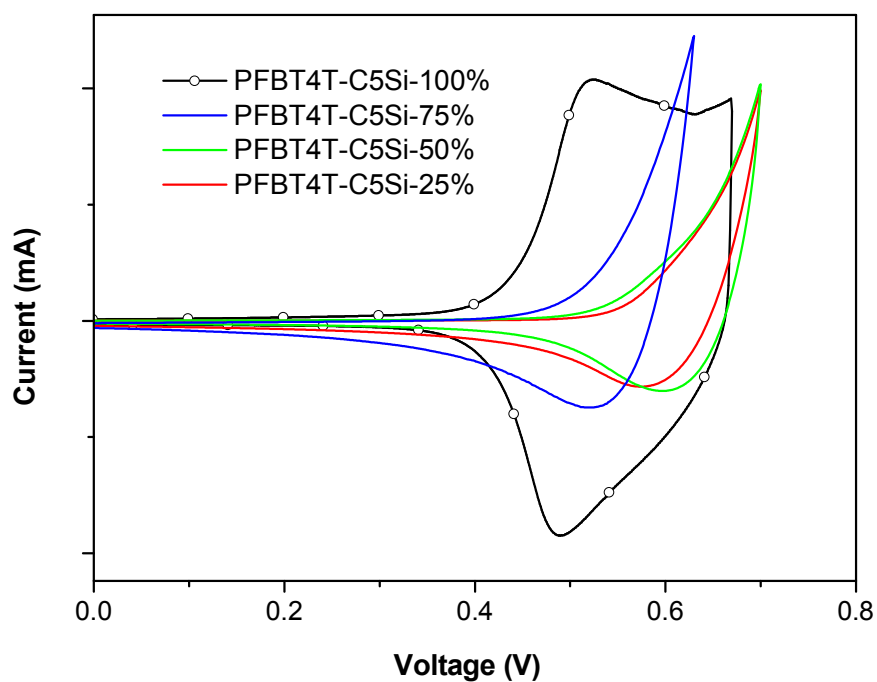


Fig. S6 Cyclic voltammetry measurements for PFBT4T-C5Si-100%, PFBT4T-C5Si-75%, PFBT4T-C5Si-50%, and PFBT4T-C5Si-25%.

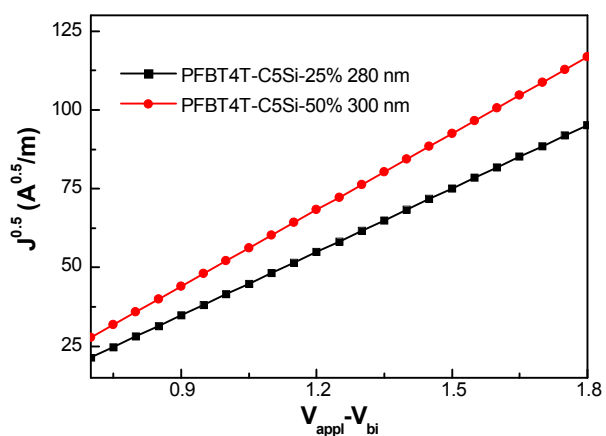


Fig. S7 SCLC $J^{1/2}$ - V characteristics of neat films of PFBT4T-C5Si-50% and PFBT4T-C5Si-25% in hole-only device: ITO/PEDOT:PSS/polymer/MoO₃/Al.

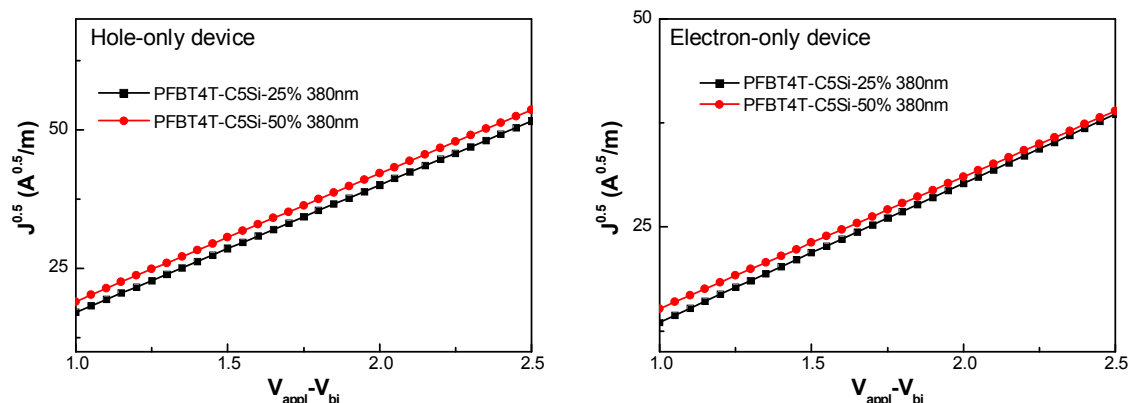


Fig. S8 SCLC $J^{1/2}$ - V characteristics of 380 nm thick blend films of PFBT4T-C5Si-50% and PFBT4T-C5Si-25% in hole-only (left) and electron-only (right) devices. Hole only device: ITO/PEDOT:PSS/polymer:PC₇₁BM (1:1.5 by weight) blend film/MoO₃/Al; electron only device: Al/polymer:PC₇₁BM (1:1.5 by weight) blend film/Ca/Al.

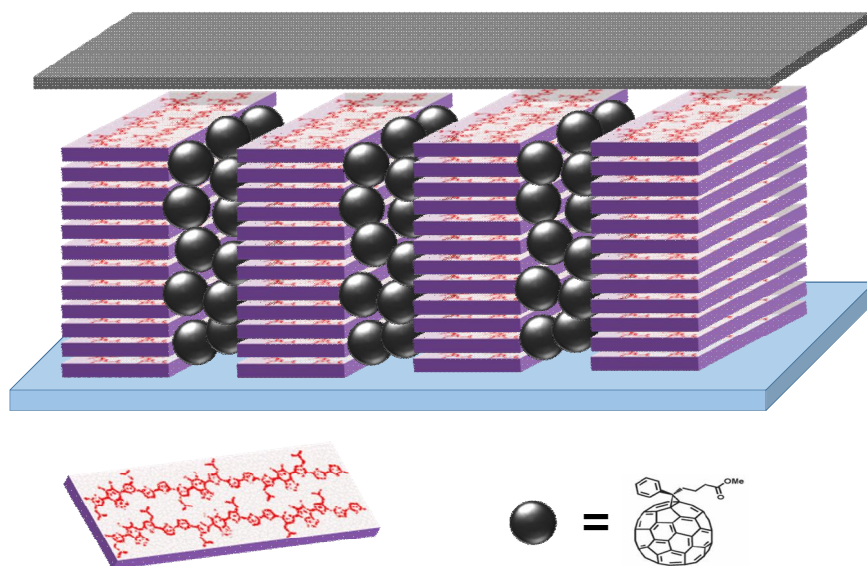


Fig. S9 An illustration for a possible model of large phase-separated bulk-heterojunction morphology with well exciton-splitting at donor/acceptor interface as well as fast hole and electron pathways. The polymer domain is of face-on orientation to vertically form thin walls with an unusual height and the acceptor domain is vertically embedded between two adjacent donor walls.

Table S1 Spin-coating conditions for active layers of PFBT4T-C5Si-50% and PFBT4T-C5Si-25%.

Polymer/PC ₇₁ BM blend film	Thickness (nm)	Polymer concentration (mg/mL)	Spin rate (rpm)
PFBT4T-C5Si-50%	270	8	700
	390	10	700
	460	11	700
PFBT4T-C5Si-25%	150	6	700
	270	8	700
	380	10	700
	420	11	700
	510	13	700
	600	14	700

Table S2. Photovoltaic performances of FBT-Th₄(1,4) based inverted polymer solar cells^a

Active layer thickness (nm)	V_{oc} (V)	J_{sc} (mA/cm ²)	FF (%)	PCE (%)
300	0.77±0.01	18.26±0.22	75.32±0.24	10.62±0.13
400	0.77±0.01	18.01±0.29	71.27±0.29	9.89±0.13
500	0.76±0.01	16.85±0.34	61.46±0.44	7.86±0.24

^a Statistic data achieved from 10 independent devices.

References

- [1] Z. Chen, P. Cai, J. Chen, X. Liu, L. Zhang, L. Lan, J. Peng, Y. Ma, Y. Cao, *Adv. Mater.*, 2014, **26**, 2586–2591.
- [2] Y. Ito, A. A. Virkar, S. Mannsfeld, J. H. Oh, M. Toney, J. Locklin, Z. Bao, *J. Am. Chem. Soc.* 2009, **131**, 9396–9404.
- [3] L. Nian, W. Zhang, N. Zhu, L. Liu, Z. Xie, H. Wu, F. Würthner, Y. Ma, *J. Am. Chem. Soc.*, 2015, **137**, 6995–6998.